Electronic Supplementary Material (ESI) for Physical Chemistry Chemical Physics.
This journal is © the Owner Societies 2021

# Supporting Information

# Magnetically induced ring currents in metallocenothiaporphyrins

Rashid R. Valiev,[a,b] Theo Kurtén,[b] Lenara I. Valiulina,[a] Sergey Yu. Ketkov,[c] Viktor N. Cherepanov,[a] Maria Dimitrova[b] and Dage Sundholm[*b]

[a] *Department of Optics and Spectroscopy, Tomsk State University, Tomsk, 634050, Russia*
[b] *Department of Chemistry, Faculty of Science, University of Helsinki, FIN-00014, Helsinki, Finland*
[c] *Laboratory of Structures of Organometallic and Coordination Compounds, G.A.Razuvaev Institute of Organometallic Chemistry, RAS 49 Tropinin St. Nizhny Novgorod 603950, Russia*

[*] Corresponding author: sundholm@chem.helsinki.fi

## 1. Bond lengths

**Table S1**. The average bond lengths (in Å) between the metal and the C atoms of the cyclopentadienyl rings.

| Metal | $(C_5H_5)_2MP$ | | | | $H_2$-$(C_5H_5)_2MP$ | | | |
|---|---|---|---|---|---|---|---|---|
| | Singlet | Triplet | Quartet | Sextet | Singlet | Triplet | Quartet | Sextet |
| V | 2.25 | 2.315 | 2.314 | | 2.244 | 2.313 | 2.316 | |
| Cr | 2.225 | 2.222 | | | 2.212 | 2.206 | | |
| Mn | 2.155 | 2.175 | | 2.416 | 2.145 | 2.222 | | 2.427 |
| Fe | 2.086 | 2.098 | | | 2.090 | 2.110 | | |
| Co | 2.079 | 2.110 | | | 2.102 | 2.288 | | |
| Ni | 2.195 | 2.229 | | | 2.376 | 2.258 | | |
| Mo | 2.317 | 2.333 | | | 2.297 | 2.331 | | |
| Tc | 2.239 | 2.276 | | 2.335 | 2.246 | 2.292 | | 2.488 |
| Ru | 2.209 | 2.212 | | | 2.217 | 2.221 | | |
| Rh | 2.219 | 2.231 | | | 2.247 | 2.253 | | |

## 2. Relative energies

**Table S2**. The relative energy (in kcal/mol) between the singlet and triplet states of the studied molecules.

| Metal | $(C_5H_5)_2MP$ | | $H_2$-$(C_5H_5)_2MP$ | |
|---|---|---|---|---|
| | Singlet | Triplet | Singlet | Triplet |
| $V^+$ | 21.71 | 0 | 30.48 | 0 |
| Cr | 29.49 | 0 | 23.59 | 0 |
| $Mn^+$ | 24.13 | 0 | 18.02 | 0 |
| Fe | 0 | 12.02 | 0 | 17.84 |
| $Co^+$ | 0 | 7.58 | 0 | 9.13 |
| Ni | 4.42 | 0 | 8.14 | 0 |
| Mo | 2.06 | 0 | 10.23 | 0 |
| $Tc^+$ | 2.08 | 0 | 0 | 2.19 |
| Ru | 0 | 13.20 | 0 | 20.23 |
| $Rh^+$ | 0 | 10.04 | 0 | 22.78 |

## 3. Electron configuration of metallocenes

Table S3. Ground-state electron configuration of neutral and cationic metallocenes ($Cp_2M$).

| $Cp_2M$ | Neutral | Cation |
|---|---|---|
| V | $(e_2')^2(a_1')^1(e_1'')^0\,(^4A_2')$ | $(e_2')^2(a_1')^0(e_1'')^0\,(^3A_2')$ |
| Cr | $(e_2')^3(a_1')^1(e_1'')^0\,(^3E_2')$ | $(e_2')^2(a_1')^1(e_1'')^0\,(^4A_2')$ |
| Mn | $(e_2')^2(a_1')^1(e_1'')^2(^6A_1')$ | $(e_2')^2(a_1')^1(e_1'')^1\,(^5E_1'')$ |
| Fe | $(e_2')^4(a_1')^2(e_1'')^0\,(^1A_1')$ | $(e_2')^3(a_1')^2(e_1'')^0\,(^2E_2')$ |
| Co | $(e_2')^4(a_1')^2(e_1'')^1\,(^2E_1'')$ | $(e_2')^4(a_1')^2(e_1'')^0\,(^1A_1')$ |
| Ni | $(e_2')^4(a_1')^2(e_1'')^2\,(^3A_2')$ | $(e_2')^4(a_1')^2(e_1'')^1\,(^2E_1'')$ |

## 4. Ring-current strengths

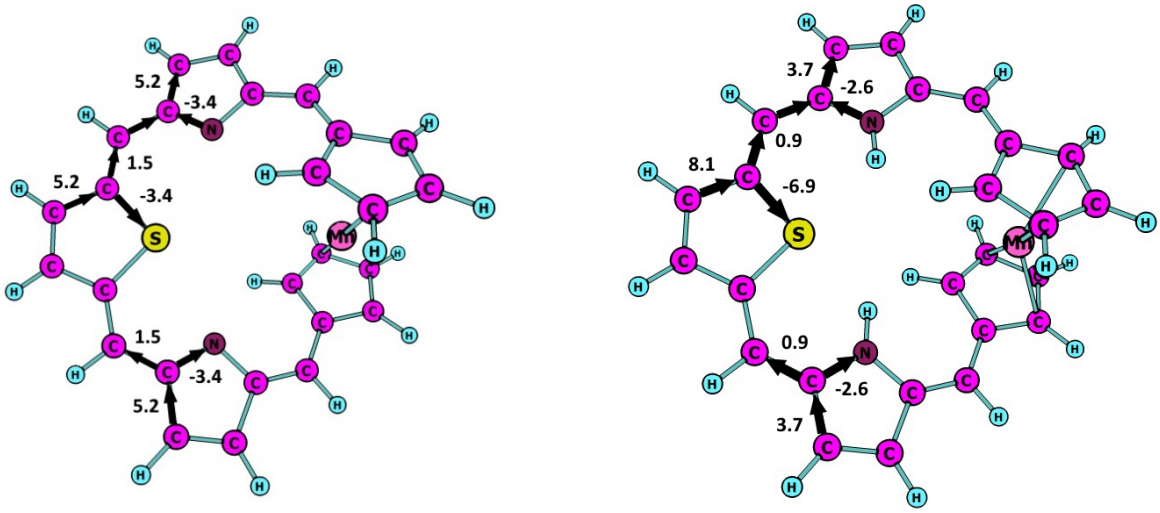


**Figure S1.** The strength of the ring current (in nA/T) passing along selected bonds of (a) the sextet state of $(C_5H_5)_2MnP$ and (b) of the sextet state of $H_2$-$(C_5H_5)_2MnP$.

# 5. Streamline representations of the magnetically induced current density

## 5.1. $H_2$-$(C_5H_5)_2$FeP

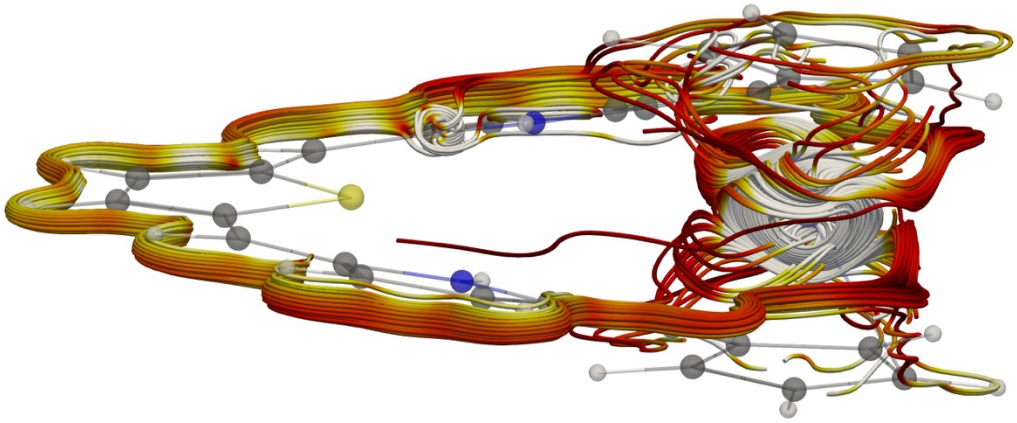

**Figure S2.** A streamline representation of the global diatropic magnetically induced current-density pathway in $H_2$-$(C_5H_5)_2$FeP outside the skeleton of the molecule.

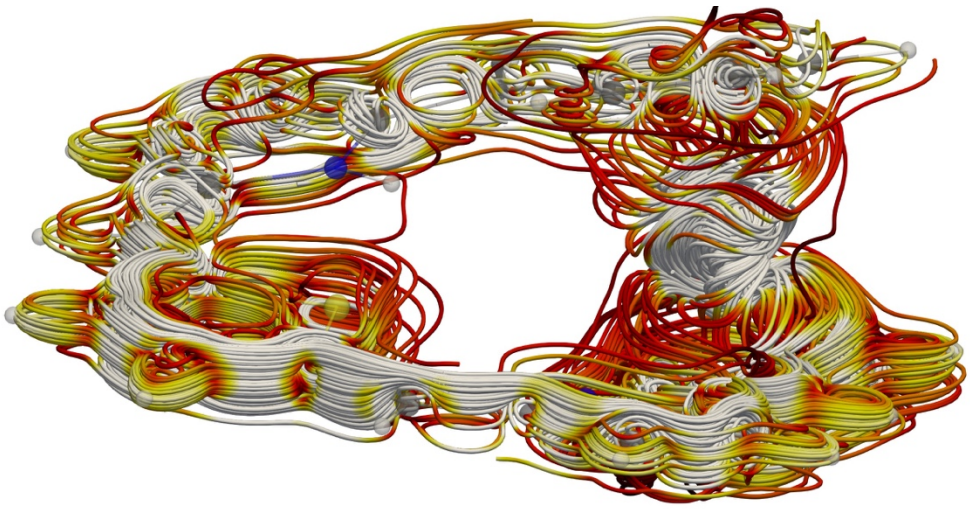

**Figure S3.** A streamline representation of the global diatropic magnetically induced current-density pathway in $H_2$-$(C_5H_5)_2$FeP at the skeleton of the molecule.

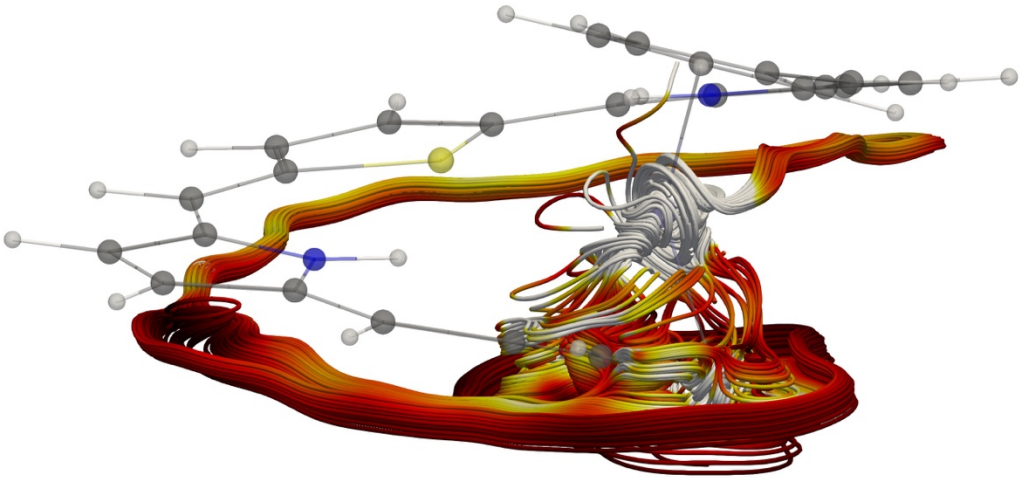

**Figure S4.** A streamline representation of the global diatropic magnetically induced current-density pathway in $H_2$-$(C_5H_5)_2$FeP on one side of the molecule.

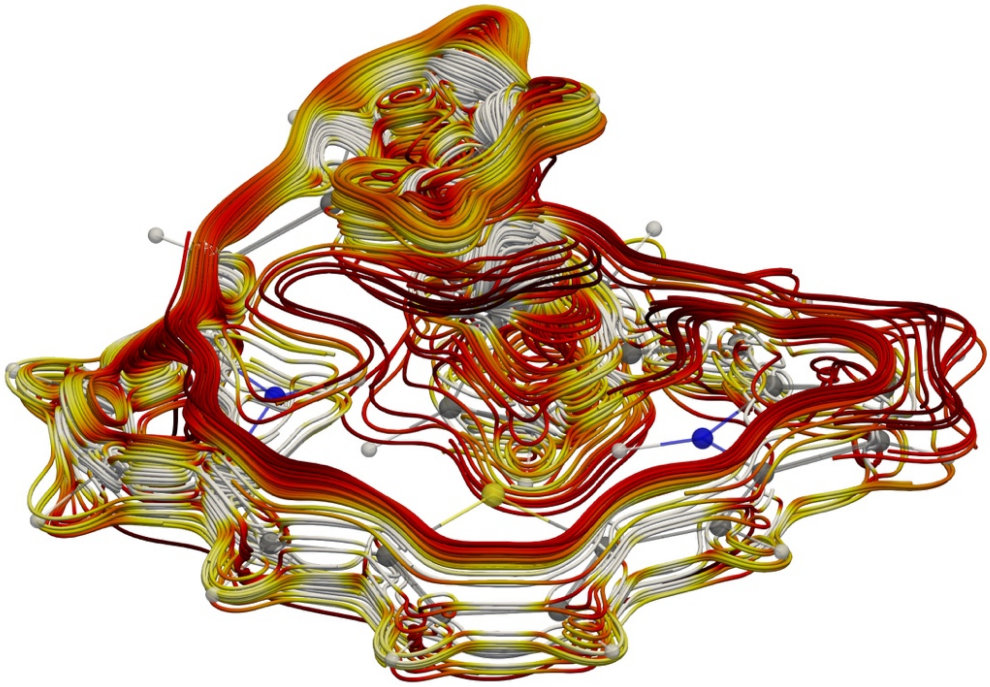

**Figure S5.** A streamline representation of the global diatropic magnetically induced current-density pathway in $H_2$-$(C_5H_5)_2$FeP passing over the ferrocene moiety.

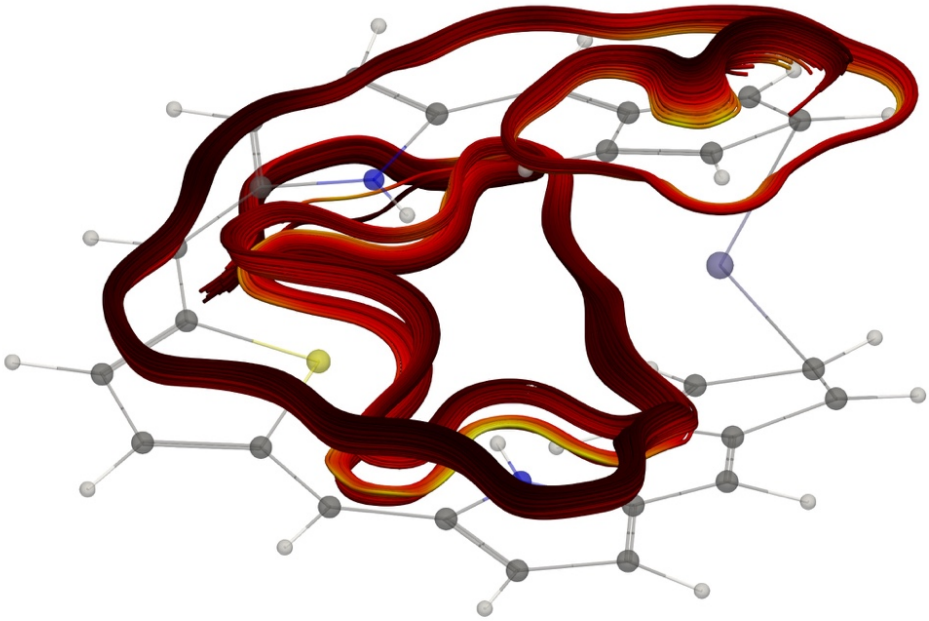

**Figure S6.** A streamline representation of the global paratropic magnetically induced current-density pathway in $H_2$-$(C_5H_5)_2$MnP on one side of the molecule.

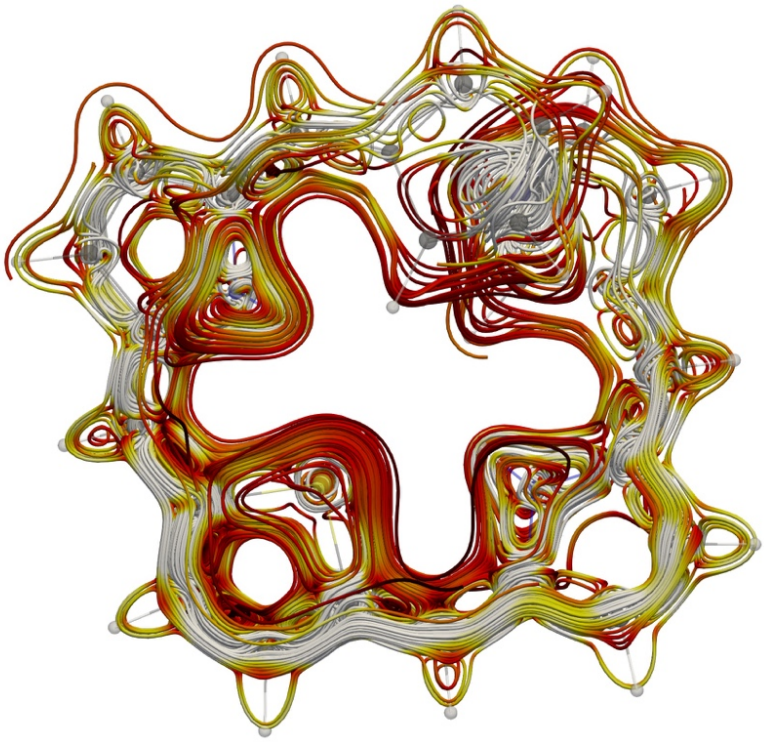

**Figure S7.** A streamline representation of the global magnetically induced current-density pathways in $H_2$-$(C_5H_5)_2FeP$, top view.

## 5.2. $(C_5H_5)_2FeP$

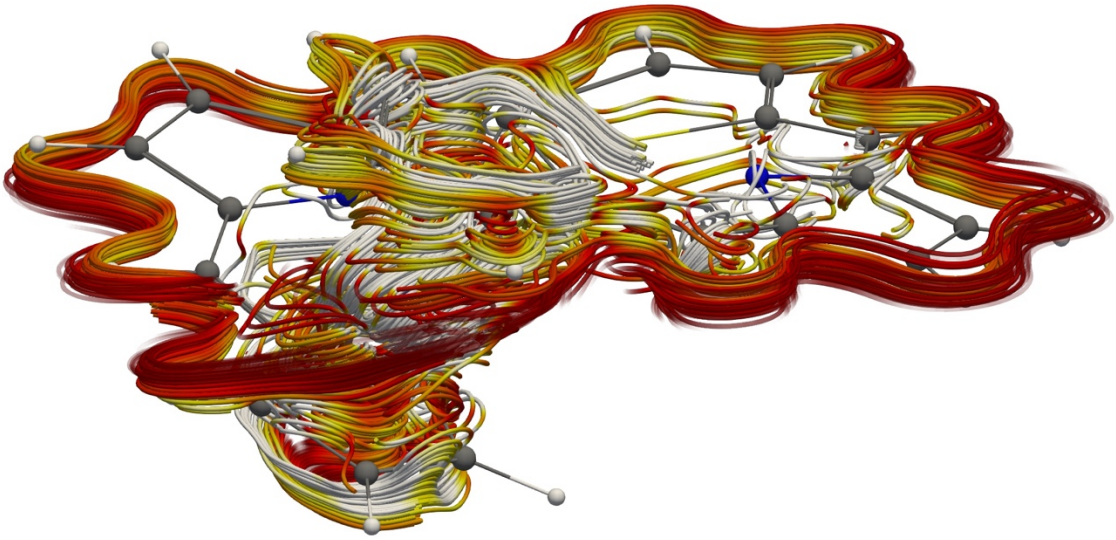

**Figure S8.** A streamline representation of the global diatropic magnetically induced current-density pathway in $(C_5H_5)_2FeP$ outside the skeleton of the molecule.

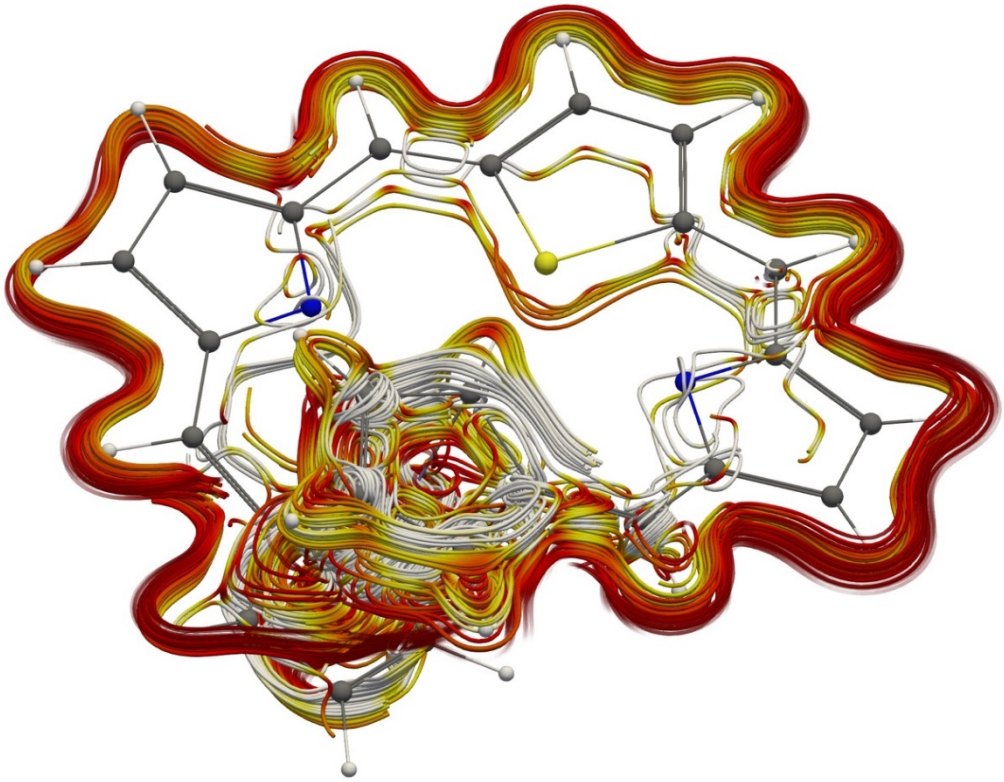

**Figure S9.** A streamline representation of the global diatropic magnetically induced current-density pathway in $(C_5H_5)_2FeP$ outside the skeleton of the molecule.

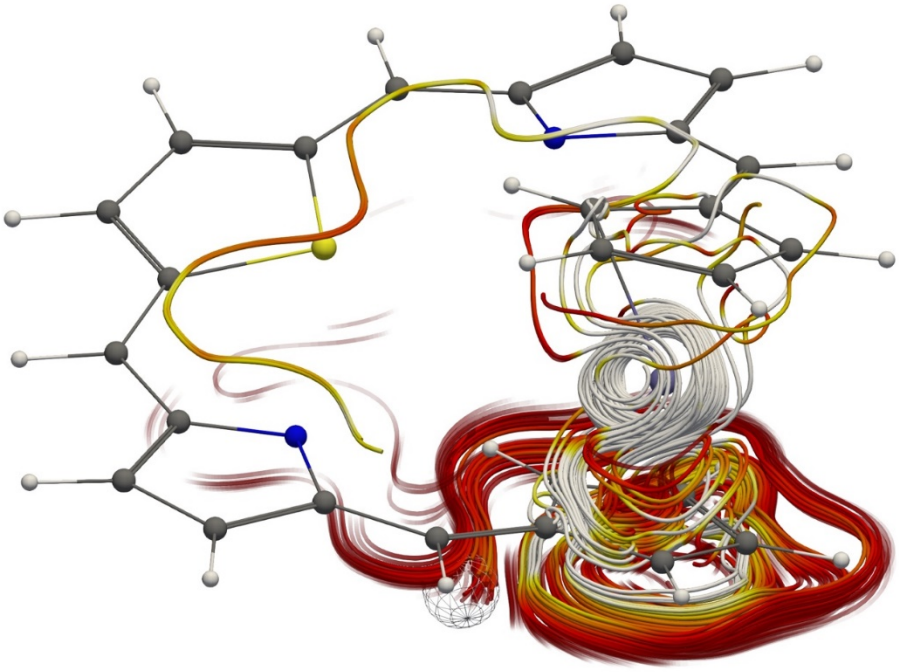

**Figure S10.** A streamline representation of the global paratropic magnetically induced current-density pathway in $(C_5H_5)_2FeP$ extending over the ferrocene unit, side view.

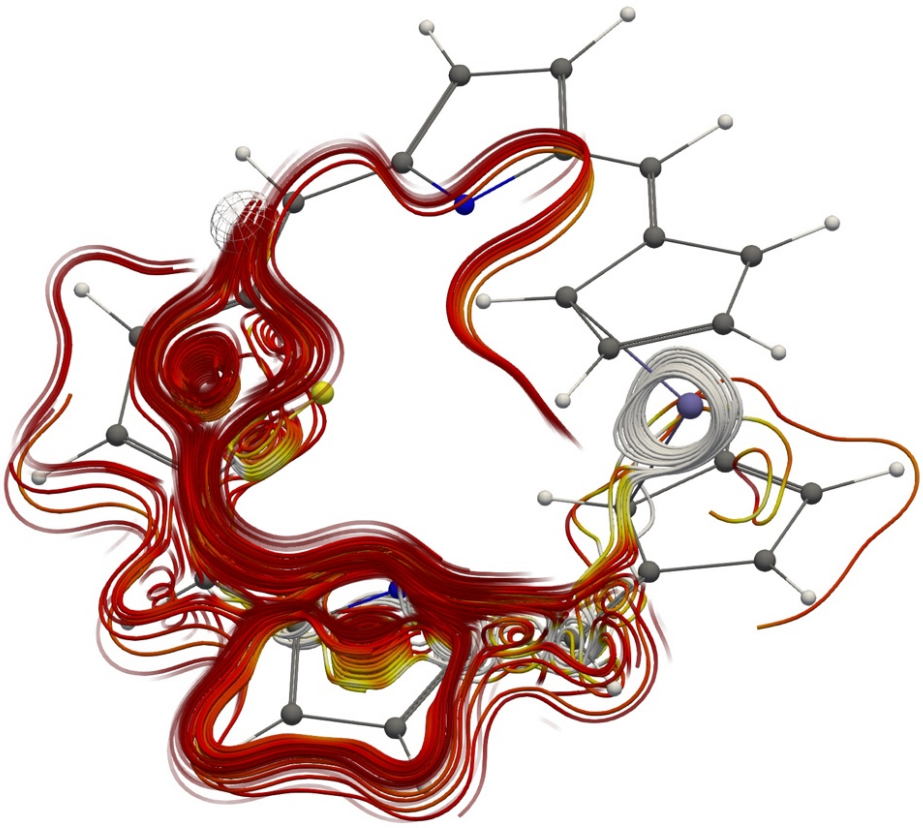

**Figure S11.** A streamline representation of the global paratropic magnetically induced current-density pathway in $(C_5H_5)_2FeP$ splitting at the thiophene unit into an inner and an outer pathway.

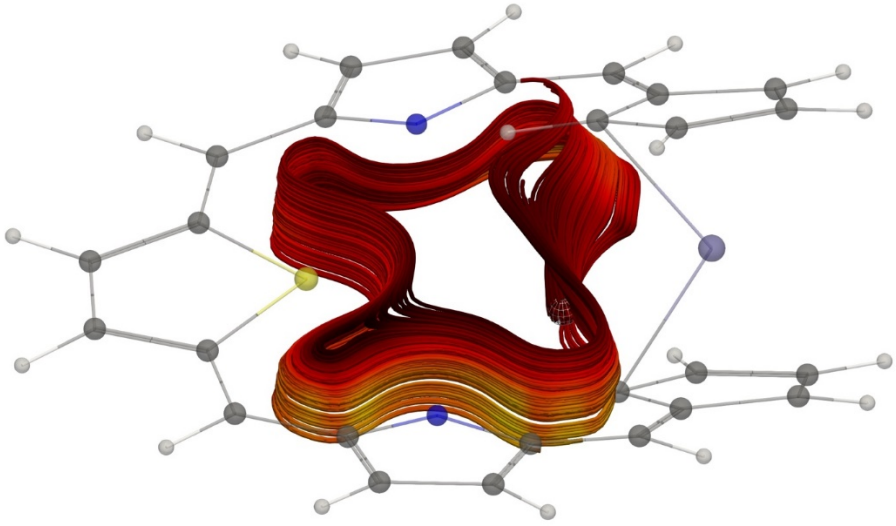

**Figure S12.** A streamline representation of the global paratropic magnetically induced current-density pathway in $(C_5H_5)_2FeP$ on the inner perimeter of the molecule.